Investigation of structural and thermal evolution in novel layered perovskite NdSrMn<inf>2</inf>O<inf>5</inf>+<inf>δ</inf> via neutron

Hindawi
International Journal of Chemical Engineering
Volume 2020, Article ID 6642187, 7 pages
https://doi.org/10.1155/2020/6642187

Research Article

Investigation of Structural and Thermal Evolution in Novel Layered Perovskite $NdSrMn_2O_{5+\delta}$ via Neutron Powder Diffraction and Thermogravimetric Analysis

Shammya Afroze,[1,2] Duygu Yilmaz,[2] Md Sumon Reza,[1] Paul F. Henry,[3,4] Quentin Cheok,[1] Juliana H Zaini,[1] Abul K. Azad,[1] Alibek Issakhov,[5] and Milad Sadeghzadeh[6]

[1]*Faculty of Integrated Technologies, Universiti Brunei Darussalam, Jalan Tungku Link, Gadong, BE 1410, Bandar Seri Begawan, Brunei Darussalam*
[2]*Department of Chemistry and Chemical Engineering, Chalmers University of Technology, SE 412 96, Gothenburg, Sweden*
[3]*ISIS Pulsed Neutron & Muon Facility, Rutherford Appleton Laboratory, Harwell Campus, OX11 0QX, Didcot, UK*
[4]*Department of Chemistry–Ångström Laboratory Inorganic Chemistry, Uppsala University, 751 21 Uppsala, Sweden*
[5]*Faculty of Mechanics and Mathematics, Department of Mathematical and Computer Modelling, Al-Farabi Kazakh National University, Almaty, Kazakhstan*
[6]*Department of Renewable Energy and Environmental Engineering, University of Tehran, Tehran, Iran*

Correspondence should be addressed to Abul K. Azad; abul.azad@ubd.edu.bn and Milad Sadeghzadeh; milad.sadeghzadeh@gmail.com

Received 17 October 2020; Revised 28 October 2020; Accepted 16 November 2020; Published 29 November 2020

Academic Editor: Mohammad Hossein Ahmadi

Neutron diffraction is one of the best methods for structural analysis of a complex, layered perovskite material with low symmetry by accurately detecting the oxygen positions through octahedral tilting. In this research, the crystal structure of $NdSrMn_2O_{5+\delta}$ was identified through X-ray diffraction (XRD) and neutron powder diffraction (NPD) at room temperature (RT), which indicated the formation of a layered structure in orthorhombic symmetry in the *Pmmm* (no. 47) space group. Rietveld refinement of the neutron diffraction data has confirmed the orthorhombic symmetry with unit cell parameters ($a = 3.8367$ (1) Å, $b = 3.8643$ (2) Å, and $c = 7.7126$ (1) Å), atomic positions, and oxygen occupancy. Thermogravimetric analysis revealed the total weight loss of about 0.10% for 20–950°C temperature, which occurred mainly to create oxygen vacancies at high temperatures. Rietveld analyses concurred with the XRD and neutron data allowing correlation of occupancy factors of the oxygen sites.

1. Introduction

The perovskite materials are used widely in solid oxide fuel cells (SOFCs) due to its diversity in chemical compositions. Ideal cubic symmetrical perovskite oxides have the general formula ABO_3 [1], where A and B indicate A-site and B-site cations and O is the anion [2]. Perovskite oxides containing excess oxygen due to interstitial oxygen atoms are unstable thermodynamically [3, 4]. Since oxygen has a high electronegativity, it will always attract electrons from heated-site and B-site cations and make them mixed-valence state for stability. As a result, research is being concentrated on perovskite oxides which have oxygen deficiency, and this deficiency can be created by manipulating the cationic and anionic stoichiometry of ABO_3 [5]. In recent times, the layered perovskites have attracted researchers because of their promising properties in energy sectors [6–8]. Rare-earth perovskites, such as $PrBaMn_2O_5$ and $NdBaMn_2O_5$, exhibited excellent redox stability (this implies that more easily reduced perovskite exhibits higher catalytic activity) and tolerance to coking and sulfur contamination from fuels [9]. Besides, some manganese-based layered perovskite can

be used as oxygen storage materials in solid oxide fuel cells (SOFCs) [10] and solid oxide electrolyzer cells (SOECs) due to their electron-conductive nature [11–13]. Some layered-type perovskites used as electrodes in SOFCs [14–18] fueled through hydrogen or other syngas [19–22] have also shown promising results.

The structural distortion is our core consideration as it affects the physical and electrochemical properties of the perovskite-type oxides [23–25]. Neutron diffraction is a robust technique that can determine complex crystal structure, oxygen stoichiometry, and oxygen vacancy ordering. It is noteworthy that the neutron is scattered from the nuclei of the atoms allowing for the formation of different isotopes of the same atom and could detect light atoms masked by the heavy atoms [26]. The Bragg reflections of the powder pattern with a long Q-range can easily be detected. Many efforts have been dedicated to enriching the performance of layered perovskite by substituting various cations, especially Mn-doped rare-earth perovskite. As an anode for SOFCs, $(PrBa)_{0.95}(Fe_{0.9}Mo_{0.1})_2O_{5+\delta}$ (PBFM) demonstrated a high power density of 1.72 $W{\cdot}cm^{-2}$ at 800°C (as reported in [27]), whereas the composition $SmBaCo_{0.5}Mn_{1.5}O_{5+\delta}$ demonstrated a power density of 377 mW/cm^2 and $SmBaMn_2O_{5+\delta}$ exhibited high power density of 782 $mW{\cdot}cm^{-2}$ at 900°C as an electrode [16, 28].

The synthesis of a novel material was elaborately discussed, and the results of high-resolution neutron powder diffraction (NPD) studies were observed on the crystallized sample in this work. We report the complete structural data of these materials and describe the thermal properties from thermogravimetric analysis.

2. Materials and Methods

The solid-state synthesis technique [18, 29–33] was applied to developing $NdSrMn_2O_{5+\delta}$. Oxide powders of Nd_2O_3 (≥99.90%, Sigma-Aldrich), $SrCO_3$ (≥99.90%, Aldrich), and MnO (≥99.50%, Aldrich) were weighed according to their stoichiometric ratios and ground with the aid of a mortar and pestle using ethanol as a reagent [34]. The powders were calcined at 1000°C for 10 hours after drying. The powders were pressed into pellets and sintered at 1200°C for 12 hours with 5°C·min^{-1} heating and cooling rate with intermediate grinding. Subsequently, the pellets were reground and resintered at 1400°C for another 12 hours. The whole synthesis process was operated under an Argon (Ar) atmosphere with a gas flow rate of 40 $ml{\cdot}min^{-1}$. X-ray powder diffraction (XRD) and neutron powder diffraction (NPD) were used to analyze the crystal structure of $NdSrMn_2O_{5+\delta}$ material.

The phase structure was first determined by XRD using a Bruker axs-D8 Advance diffractometer. Data were collected in the 2θ range from 10° to 79.995° with increments of 0.02° per second. The Rietveld refinement procedure was used to analyze the XRD data [35] using the Fullprof software [36]. A polynomial function (6-coefficient) was set for the background, and the pseudo-Voigt function was used to model the peak shapes.

Neutron powder diffraction data were collected at room temperature (RT) with the Polaris diffractometer (medium-resolution powder diffractometer at a high intensity) at the ISIS Neutron & Muon Source, UK [37, 38]. The time-of-flight (TOF) powder diffraction data were analyzed using GSAS-II [39] software. This material is debuted under the *Pmmm* space group through the Rietveld analysis of the high-resolution NPD data; a layered perovskite structure was formed. The Rietveld analysis used standard parameters for the refinement: a shifted Chebyshev series as background as instigated in GSAS software, zero shift, scale factor, profile parameters (type 3 in GSAS), cell parameters, atomic coordinates, site-occupancy factor (SOF), and atomic displacement factors (ADP).

To perform thermogravimetric analysis (TGA), a Netzsch-Gerätebau GmbH-STA 409 PC Luxx Simultaneous Thermal Analyzer was used to perceive the weight change with increasing temperature under flowing nitrogen. 99.51 mg of $NdSrMn_2O_{5+\delta}$ powder was placed in a ceramic crucible (Al_2O_3 DSC/TG pan) and heated from 20 to 950°C at a rate of 5°C·min^{-1} under 20 $ml{\cdot}min^{-1}$ of N_2 flow. An isothermal hold for 1 hour removed absorbed species before cooling. The process was then repeated to ensure complete desorption of any contaminants. Upon complete desorption, N_2 flow was substituted for airflow, and the mass change were recorded until equilibrium was reached.

3. Results and Discussion

Solid-state reaction methods have been used to prepare the layered perovskite $NdSrMn_2O_{5+\delta}$. This layered perovskite is challenging to develop in a pure form, but the single-phase was obtained. Our synthesis method was also different from the method used to obtain $NdBaMn_2O_{5+\delta}$ [40] but similar to the synthesis process for $PrSrMn_2O_{5+\delta}$ [30]. Figure 1 shows the XRD pattern for $NdSrMn_2O_{5+\delta}$ sintered at 1400°C under Ar atmosphere. Some extra small peaks could not be indexed with the basic unit cell pattern. But, most of the peaks in Figure 1 can be indexed to an orthorhombic unit cell. The crystalline structure of this material was determined as ceramic through the XRD pattern. The XRD for the sample was measured at room temperature.

Fundamental understanding of the structure of the $NdSrMn_2O_{5+\delta}$ sample was investigated by neutron powder diffraction at room temperature. Oxygen vacancies are created in the material, which can balance the total charge. The single-phase orthorhombic structure was obtained from neutron diffraction with the space group, *Pmmm*. Rietveld refinement of room-temperature NPD data (Figure 2) revealed that $NdSrMn_2O_{5+\delta}$ achieved cell parameters $a = 3.8367$ (1) Å, $b = 3.8643$ (2) Å, and $c = 7.7126$ (1) Å with dimensions $a_p \times a_p \times 2a_p$ as observed in $NdBaCo_{2-x}Mn_xO_{5+\delta}$ [12]. Bank 2 (up to 7 Å) NPD data were analyzed via Rietveld refinement. The space groups, refinement factors (*R*-factors), and cell parameters are listed in Table 1, and atomic positions, Wyckoff positions, and isotropic temperature factors are listed Table 2, respectively. In Table 1, the other layered perovskite structures were compared with the present work.

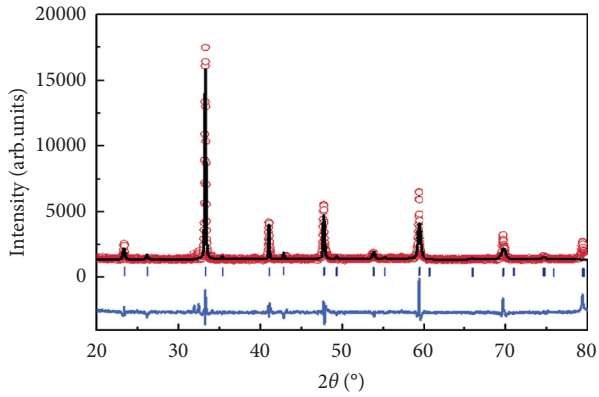

Figure 1: Rietveld refinement pattern of $NdSrMn_2O_{5+\delta}$ for XRD.

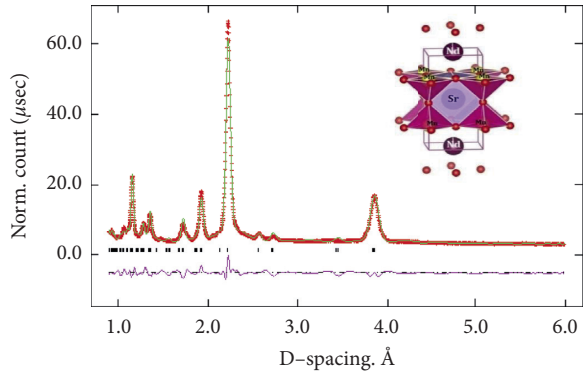

Figure 2: Rietveld refinement profile of $NdSrMn_2O_{5+\delta}$ at room temperature with 3D polyhedral representation. The red line depicts the original data, the continuous green line depicts the calculated profile data, and the purple bottom line depicts the difference.

Table 1: Comparison of the results obtained from the Rietveld analysis of NPD data for $NdSrMn_2O_{5+\delta}$ at RT (space group, *Pmmm*) with other data from the literature.

Parameters	$NdSrMn_2O_{5+\delta}$ at RT	$NdBaMn_2O_{5+\delta}$ at 25°C*	$YBaMn_2O_5$ at 25°C**	$PrSrMn_2O_{5+\delta}$ at RT***
Structure model	Orthorhombic	Tetragonal	Tetragonal	Orthorhombic
Space group	*Pmmm*	*P4/nmm*	P4/mmm	*Pmmm*
Volume (Å^3)	416.8110	—	—	480.9290
R-factors				
R_f (%)	5.50	—	—	—
R_p (%)	4.87	2.21	—	—
R_{wp} (%)	6.86	—	6.00	—
Cell parameters				
a (Å)	3.8367 (1)	5.6140 (1)	3.9186 (2)	3.8906 (1)
b (Å)	3.8643 (2)	5.6140 (1)	3.9186 (2)	3.8227 (1)
c (Å)	7.7126 (1)	7.7430 (2)	7.6540 (5)	7.6846 (2)

*$NdBaMn_2O_{5+\delta}$ [41], **$YBaMn_2O_5$ [42], ***$PrSrMn_2O_{5+\delta}$ [30].

The oxygen occupation was fixed at 1 at three oxygen sites for the space group *Pmmm*, O1, O2, and O3, repectively. These three sites remained locked in the Rietveld model refinement to detect the significant eccentricity from unity. No significant changes were found for three sites. U_{iso} as the thermal vibration parameters for Nd, Sr, and Mn were refined isotropically. These sites were set isotropically to get a standard deviation. Atomic displacement parameters (ADP) and the site-occupancy factors (SOF) correlated with each other. As a result, they were unable to be refined simultaneously. DIFA (a small correction in GSAS software to allow a reflection in the expected time-of-flight peak shifts due to sampling absorption), absorption, and scaling parameters were constrained in this case. The isotropic thermal

Table 2: List of Wyckoff positions, atomic positions, and isotropic temperature factors for $NdSrMn_2O_{5+\delta}$ (space group, *Pmmm*) from neutron diffraction data at RT.

Atoms	Wyckoff positions	x	y	z	U_{iso}
Nd	1f	0.5000	0.5000	0.0000	0.0231 (1)
Sr	1h	0.5000	0.5000	0.5000	0.0172 (1)
Mn	2q	0.0000	0.0000	0.7556	0.0025 (2)
O1	2r	0.0000	0.5000	0.2438	0.0417 (1)
O2	2s	0.5000	0.0000	0.2478	0.0350 (3)
O3	1c	0.0000	0.0000	0.5000	0.0166 (1)

vibration parameters (U_{iso}) also remained constrained in each phase. The average B-O bond lengths at room temperature can be compared to the calculated ionic radii by Shannon [43], where <Mn-O> is 1.9218 (6) Å (calc. 2.08 Å). Main bond distances and their average distances are tabulated in Table 3.

The surface morphology exhibits well-connected, large grains showing visible grain growth with an orthorhombic form. There were no secondary phases found at the grain boundary region in the $NdSrMn_2O_{5+\delta}$ sample. The grains were approximately 10 μm in size for the sample. The porous morphology (Figure 3) depicted that this material can be used as an electrode for fuel cells, the pores will assist the conduction of electrons, as well as allow fuel to pass easily through the structure [44].

An inert atmosphere is needed during the thermogravimetric experiment to prevent oxidation of the sample during thermal treatment. A vacuum environment was created inside the TGA-differential scanning calorimetry (DSC) chamber to ensure an utterly anoxic environment for the analysis. A small amount of the sample $NdSrMn_2O_{5+\delta}$ was taken for thermogravimetric analysis- (TGA-) differential scanning calorimetry (DSC) under a nitrogen environment. TGA showed that oxidation occurred at 200°C while heating in a single gradation (Figure 3) including weight loss with 1 oxygen atom in the formula unit. A small amount of weight loss was observed from 20°C to 950°C in the TGA-DSC curve in N_2 atmosphere. But, there no phase transition occurred which is seen in the DSC curve as there is no exo- or endothermic peaks observed in Figure 3 [45]. The weight loss occurred due to evaporation of the moisture [46], formation of oxygen vacancy, and valence state of cations [3]. In the first step (200°C–500°C), the weight loss was high due to the moisture evaporation [47], and the decline in this region was about 0.084%. Above 500°C, the weight loss was less because all the organic compounds and all other elements end up in this step and the sample behaves as a thermally stable material [48–53]; from 500°C to 950°C, the weight loss was approximately 0.016%. The total weight loss observed was about 0.10% for a temperature range between 20 and 950°C which is comparable with other perovskite materials; $SmBaMn_2O_{5+\delta}$ (0.036%) [54] and $PrSrMn_2O_{5+\delta}$ [30]. The oxygen content of the equilibrium stage decreases with temperature leading to oxygen vacancy formation during TGA-DSC. Table 4 shows that the calculated oxygen occupancy values from TGA are very close to the calculated values from Rietveld refinement. From Table 4, we can see

Table 3: Leading bond distances (Å) ($d \leq 6$ Å) for orthorhombic $NdSrMn_2O_{5+\delta}$ determined from NPD data at room temperature (RT).

Parameters	Bond length (Å)
Nd-O1 (×4)	2.6943 (4)
Nd-O2 (×4)	2.7044 (4)
<Nd-O>	2.6993 (5)
Sr-O1 (×4)	2.7614 (5)
Sr-O2 (×4)	2.7322 (4)
Sr-O3 (×4)	2.7233 (4)
<Sr-O>	2.7389 (6)
Mn-O1 (×4)	1.9200 (4)
Mn-O2 (×4)	1.9325 (4)
Mn-O3 (×4)	1.9131 (5)
<Mn-O>	1.9218 (6)

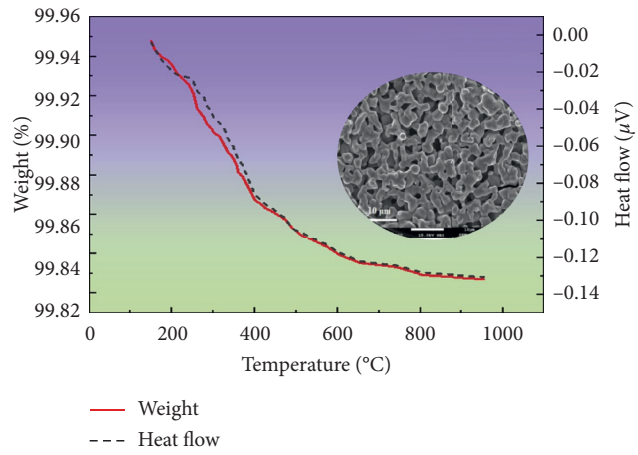

Figure 3: TGA plot of $NdSrMn_2O_{5+\delta}$ on heating from 20°C to 950°C. Single-phase SEM morphology of $NdSrMn_2O_{5+\delta}$ inserted.

that due to the fewer changes in oxygen occupancy in the $NdSrMn_2O_{5+\delta}$ crystal powder, a minimal weight loss has been observed which is close to or less than other layered structures from the literature that are comparable.

The crystal structure of $NdSrMn_2O_{5+\delta}$ is an example of layered orthorhombic symmetry, where both B-cations occupy the perovskite-like corner-shared octahedral (MnO_1 and MnO_2) sites. In this study, we evaluated the structural and thermal characteristics. According to these characterizations, we obtained a good result due to its high porosity, stable structure, and sufficient oxygen deficiency in comparison to similar types of layered perovskites. For $NdSrMn_2O_{5+\delta}$, the Rietveld analysis indicates that all oxygen vacancies occur in the O1 and O2 sites. The volume of this $NdSrMn_2O_{5+\ \delta}$ material is not so large without any long-range ordering in B-site which indicates an oxygen-deficient layered perovskite oxide. During TGA-DSC, when the heating starts, the weight loss was mainly observed from 200 to 950°C on account of increasing oxygen deficiency and thermally stable [55] due to its minimal amount of weight loss. Also, similar rare-earth layered perovskite has already given a promising result with the same space group for IT-

Table 4: Comparison of TGA results for $NdSrMn_2O_{5+\delta}$ and perovskite structures in the literature.

Compositions	Temperature (°C)	Oxygen occupancy from Rietveld refinement	Weight change (% TG)	Calculated oxygen occupancy from TGA	Ref.
$NdSrMn_2O_{5+\delta}$	20- 950	5.3829	0.1005	5.3994	This study
$SmBaMn_2O_{5+\delta}$	Up to 1000	—	0.0220	—	[54]
$PrBaMn_2O_{5+\delta}$	25- 800	—	—	—	[25]
$PrSrMn_2O_{5+\delta}$	20- 1000	—	0.3600		[30]

SOFC [56]. These types of layered perovskites have recently gained a great deal of attention for SOFC anode materials because of their unusually high oxygen transport kinetics rate [57, 58]. It is established that the layered perovskite performs well for fuel cells reported by Abdalla et al. [40, 54].

4. Conclusions

Terminally, the solid-state synthesis method was used to prepare this single-phase novel, layered perovskite $NdSrMn_2O_{5+\delta}$. XRD, NPD, and TGA-DSC analyses were used to determine structural and thermal properties. Both XRD and NPD data confirmed that the sample crystallizes in orthorhombic symmetry with the space group, *Pmmm* via Rietveld analysis. The structural features of this orthorhombic structure were measured by the action of flowing nitrogen (N_2) with temperature and time, evidenced by a minimal weight loss (0.1%), which may be the weight loss attributed to the oxygen vacancy formation or a decrease in oxygen content. The minimal weight loss occurred in the TGA-DSC results, mainly for the fewer variations in oxygen occupancy in the $NdSrMn_2O_{5+\delta}$ crystal, whose value is closer to the results of oxygen occupancy in neutron refinement analysis. The development of layered perovskite remains an appealing research topic, and promising technology has emerged to improve SOFCs with further electrochemical experiments.

Nomenclature

δ:	Oxygen nonstoichiometry
U_{iso}:	Thermal vibrational parameters
R_p, R_{wp}, and R_f:	Residual factors or *R*-factors
SOFC:	Solid oxide fuel cell
SOEC:	Solid oxide electrolyzer cell
XRD:	X-ray powder diffraction
NPD:	Neutron powder diffraction
RT:	Room temperature
TOF:	Time of flight
SOF:	Site-occupancy factor
ADP:	Atomic displacement factors
TGA:	Thermogravimetric analysis
DSC:	Differential scanning calorimetry.

Data Availability

The data used to support the findings of this study are included within the article.

Conflicts of Interest

The authors declare that they do not have any conflicts of interest.

Acknowledgments

The author Shammya Afroze is grateful to Universiti Brunei Darussalam for awarding her by UBD Graduate Scholarship (UGS). The author is especially indebted to late Professor Sten G. Eriksson from Chalmers University of Technology, Sweden. The ISIS Neutron and Muon Facility, UK, is greatly acknowledged for its scheduled beam-time (RB1810638, DOI: https://doi.org/10.5286/ISIS.E.RB1810638).

References

[1] N. Tien Thao and L. T. Son, "Production of cobalt-copper from partial reduction of La(Co, Cu)O_3 perovskites for CO hydrogenation," *Journal of Science: Advanced Materials and Devices*, vol. 1, no. 3, pp. 337–342, 2016.

[2] S. Feraru, P. Samoila, A. I. Borhan, M. Ignat, A. R. Iordan, and M. N. Palamaru, "Synthesis, characterization of double perovskite Ca_2MSbO_6 (M=Dy, Fe, Cr, Al) materials via sol-gel auto-combustion and their catalytic properties," *Materials Characterization*, vol. 84, pp. 112–119, 2013.

[3] M. A. Peña and J. L. G. Fierro, "Chemical structures and performance of perovskite oxides," *Chemical Reviews*, vol. 101, no. 7, pp. 1981–2018, 2001.

[4] A. V. Kovalevsky, S. Populoh, S. G. Patrício et al., "Design of $SrTiO_3$-based thermoelectrics by tungsten substitution," *The Journal of Physical Chemistry C*, vol. 119, no. 9, pp. 4466–4478, 2015.

[5] Q. Ji, L. Bi, J. Zhang, H. Cao, and X. S. Zhao, "The role of oxygen vacancies of ABO_3 perovskite oxides in the oxygen reduction reaction," *Energy & Environmental Science*, vol. 13, no. 5, pp. 1408–1428, 2020.

[6] J.-H. Kim, L. Mogni, F. Prado, A. Caneiro, J. A. Alonso, and A. Manthiram, "High temperature crystal chemistry and oxygen permeation properties of the mixed ionic-electronic conductors LnBaCo[sub 2]O[sub 5+δ] (Ln=Lanthanide)," *Journal of The Electrochemical Society*, vol. 156, no. 12, p. B1376, 2009.

[7] R. A. Cox-Galhotra, A. Huq, J. P. Hodges et al., "Visualizing oxygen anion transport pathways in $NdBaCo_2O_{5+\delta}$ by in situ neutron diffraction," *Journal of Materials Chemistry A*, vol. 1, no. 9, pp. 3091–3100, 2013.

[8] S. Afroze, A. Karim, Q. Cheok, S. Eriksson, and A. K. Azad, "Latest development of double perovskite electrode materials for solid oxide fuel cells: a review," *Frontiers in Energy*, vol. 13, no. 4, pp. 770–797, 2019.

[9] S. Sengodan, S. Choi, A. Jun et al., "Layered oxygen-deficient double perovskite as an efficient and stable anode for direct hydrocarbon solid oxide fuel cells," *Nature Materials*, vol. 14, no. 2, pp. 205–209, 2015.

[10] M. J. Akhtar and R. T. A. Khan, "Structural studies of $SrFeO_3$ and $SrFe_{0.5}Nb_{0.5}O_3$ by employing XRD and XANES spectroscopic techniques," *Materials Characterization*, vol. 62, no. 10, pp. 1016–1020, 2011.

[11] S. Kumar, G. D. Dwivedi, A. G. Joshi, S. Chatterjee, and A. K. Ghosh, "Study of structural, dielectric, optical properties and electronic structure of Cr-doped $LaInO_3$ perovskite nanoparticles," *Materials Characterization*, vol. 131, pp. 108–115, 2017.

[12] T. Broux, M. Bahout, J. M. Hanlon et al., "High temperature structural stability, electrical properties and chemical reactivity of $NdBaCo_{2-x}Mn_xO_{5+\delta}$ ($0 \le x \le 2$) for use as cathodes in solid oxide fuel cells," *Journal of Materials Chemistry A*, vol. 2, no. 40, pp. 17015–17023, 2014.

[13] M. Bahout, S. S. Pramana, J. M. Hanlon et al., "Stability of $NdBaCo_{2-x}Mn_xO_{5+\delta}$ (x = 0, 0.5) layered perovskites under humid conditions investigated by high-temperature in situ neutron powder diffraction," *Journal of Materials Chemistry A*, vol. 3, no. 30, pp. 15420–15431, 2015.

[14] G. Kim, S. Wang, A. J. Jacobson, L. Reimus, P. Brodersen, and C. A. Mims, "Rapid oxygen ion diffusion and surface exchange kinetics in $PrBaCo_2O_{5+x}$ with a perovskite related structure and ordered A cations," *Journal of Materials Chemistry*, vol. 17, no. 24, p. 2500, 2007.

[15] C. Lim, A. Jun, H. Jo et al., "Influence of Ca-doping in layered perovskite $PrBaCo_2O_{5+\delta}$ on the phase transition and cathodic performance of a solid oxide fuel cell," *Journal of Materials Chemistry A*, vol. 4, no. 17, pp. 6479–6486, 2016.

[16] Y. Zhang, H. Zhao, Z. Du, K. Świerczek, and Y. Li, "High-performance $SmBaMn_2O_{5+\delta}$ electrode for symmetrical solid oxide fuel cell," *Chemistry of Materials*, vol. 31, no. 10, pp. 3784–3793, 2019.

[17] S. Afroze, M. S. Reza, Q. Cheok, J. Taweekun, and A. K. Azad, "Solid oxide fuel cell (SOFC); A new approach of energy generation during the pandemic COVID-19," *International Journal of Integrated Engineering*, vol. 12, no. 5, pp. 245–256, 2020.

[18] T.-H. Lee, K.-Y. Park, N.-I. Kim et al., "Robust $NdBa_{0.5}Sr_{0.5}Co_{1.5}Fe_{0.5}O_{5+\delta}$ cathode material and its degradation prevention operating logic for intermediate temperature-solid oxide fuel cells," *Journal of Power Sources*, vol. 331, pp. 495–506, 2016.

[19] M. S. Reza, A. Ahmed, W. Caesarendra et al., "Acacia holosericea: an invasive species for bio-char, bio-oil, and biogas production," *Bioengineering*, vol. 6, no. 2, p. 33, 2019.

[20] M. S. Reza, S. N. Islam, S. Afroze et al., "Evaluation of the bioenergy potential of invasive Pennisetum purpureum through pyrolysis and thermogravimetric analysis," *Energy, Ecology and Environment*, vol. 5, no. 2, pp. 118–133, 2020.

[21] M. S. Reza, S. Afroze, M. S. A. Bakar et al., "Biochar characterization of invasive Pennisetum purpureum grass: effect of pyrolysis temperature," *Biochar*, vol. 2, no. 2, pp. 239–251, 2020.

[22] "Full article: preparation of activated carbon from biomass and its' applications in water and gas purification, a review," 2020, https://www.tandfonline.com/doi/full/10.1080/25765299.2020.1766799.

[23] F. Tonus, M. Bahout, V. Dorcet et al., "A-site order-disorder in the $NdBaMn_2O_{5+\delta}$ SOFC electrode material monitored in situ by neutron diffraction under hydrogen flow," *Journal of Materials Chemistry A*, vol. 5, no. 22, pp. 11078–11085, 2017.

[24] A. C. Tomkiewicz, M. A. Tamimi, A. Huq, and S. McIntosh, "Structural analysis of $PrBaMn_2O_{5+\delta}$ under SOFC anode conditions by in-situ neutron powder diffraction," *Journal of Power Sources*, vol. 330, pp. 240–245, 2016.

[25] A. K. Azad, J. H. Kim, and J. T. S. Irvine, "Structural, electrochemical and magnetic characterization of the layered-type $PrBa_{0.5}Sr_{0.5}Co_2O_{5+\delta}$ perovskite," *Journal of Solid State Chemistry*, vol. 213, pp. 268–274, 2014.

[26] J. A. Alonso, M. J. Martínez-Lope, A. Aguadero, and L. Daza, "Neutron powder diffraction as a characterization tool of solid oxide fuel cell materials," *Progress in Solid State Chemistry*, vol. 36, no. 1-2, pp. 134–150, 2008.

[27] H. Ding, Z. Tao, S. Liu, and J. Zhang, "A high-performing sulfur-tolerant and redox-stable layered perovskite anode for direct hydrocarbon solid oxide fuel cells," *Scientific Reports*, vol. 5, no. 1, Article ID 18129, 2015.

[28] A. Olszewska, Y. Zhang, Z. Du et al., "Mn-rich $SmBaCo_{0.5}Mn_{1.5}O_{5+\delta}$ double perovskite cathode material for SOFCs," *International Journal of Hydrogen Energy*, vol. 44, no. 50, pp. 27587–27599, 2019.

[29] S. Afroze, N. Torino, P. F. Henry, M. S. Reza, Q. Cheok, and A. K. Azad, "Neutron and X-ray powder diffraction data to determine the structural properties of novel layered perovskite $PrSrMn_2O_{5+\delta}$," *Data in Brief*, vol. 29, Article ID 105173, 2020.

[30] S. Afroze, N. Torino, P. F. Henry, M. Sumon Reza, Q. Cheok, and A. K. Azad, "Insight of novel layered perovskite $PrSrMn_2O_{5+\delta}$: a neutron powder diffraction study," *Materials Letters*, vol. 261, Article ID 127126, 2020.

[31] A. K. M. Zakaria, M. A. Asgar, S.-G. Eriksson et al., "Preparation of Zn substituted Ni-Fe-Cr ferrites and study of the crystal structure by neutron diffraction," *Materials Letters*, vol. 57, no. 26-27, pp. 4243–4250, 2003.

[32] A. K. Azad, A. Kruth, and J. T. S. Irvine, "Influence of atmosphere on redox structure of BaCe 0.9 Y 0.1 O 2.95 - insight from neutron diffraction study," *International Journal of Hydrogen Energy*, vol. 39, no. 24, pp. 12804–12811, 2014.

[33] X. Xu, Y. Xie, S. Ni, A. K. Azad, and T. Cao, "Photocatalytic H_2 production from spinels $ZnGa_2$–Cr O_4 ($0 \le x \le 2$) solid solutions," *Journal of Solid State Chemistry*, vol. 230, pp. 95–101, 2015.

[34] S. Afroze, N. Torino, M. S. Reza et al., "Structure-conductivity relationship of $PrBaMnMoO_{6-\delta}$ through in-situ measurements: a neutron diffraction study," *Ceramics International*, vol. 47, no. 1, p. 541, 2021.

[35] R. C. Nederland, "A profile refinement method for nuclear and magnetic structures," *Journal of Applied Crystallography*, vol. 2, pp. 65–71, 1969.

[36] "FullProf Suite Homepage," 2019, https://www.ill.eu/sites/fullprof/.

[37] S. Hull, R. I. Smith, W. I. F. David, A. C. Hannon, J. Mayers, and R. Cywinski, "The Polaris powder diffractometer at ISIS," *Physica B: Condensed Matter*, vol. 180-181, pp. 1000–1002, 1992.

[38] R. I. Smith, S. Hull, M. G. Tucker et al., "The upgraded Polaris powder diffractometer at the ISIS neutron source," *Review of Scientific Instruments*, vol. 90, no. 11, pp. 115101–115113, 2019.

[39] B. H. Toby and R. B. Von Dreele, "GSAS-II: the genesis of a modern open-source all purpose crystallography software package," *Journal of Applied Crystallography*, vol. 46, no. 2, pp. 544–549, 2013.

[40] A. M. Abdalla, S. Hossain, J. Zhou et al., "$NdBaMn_2O_{5+\delta}$ layered perovskite as an active cathode material for solid oxide fuel cells," *Ceramics International*, vol. 43, no. 17, pp. 15932–15938, 2017.

[41] F. Tonus, M. Bahout, V. Dorcet et al., "Redox behavior of the SOFC electrode candidate $NdBaMn_2O_{5+\delta}$ investigated by high-temperature in situ neutron diffraction: first characterisation in real time of an $LnBaMn_2O_{5.5}$ intermediate phase," *Journal of Materials Chemistry A*, vol. 4, no. 30, pp. 11635–11647, 2016.

[42] J. A. Mcallister and J. P. Attfield, "A variable temperature neutron diffraction study of the layered perovskite $YBaMn_2O_5$," *Journal of Materials Chemistry*, vol. 8, no. 5, pp. 1291–1294, 1998.

[43] R. D. Shannon, "Revised effective ionic radii and systematic studies of interatomic distances in halides and chalcogenides," *Acta Crystallographica Section A*, vol. 32, no. 5, pp. 751–767, 1976.

[44] A. Sciazko, Y. Komatsu, T. Shimura, and N. Shikazono, "Multiscale microstructural evolutions of nickel-gadolinium doped ceria in solid oxide fuel cell anode," *Journal of Power Sources*, vol. 478, Article ID 228710, 2020.

[45] J. Wang, F. Meng, T. Xia et al., "Superior electrochemical performance and oxygen reduction kinetics of layered perovskite $PrBa_xCo_2O_{5+\delta}$ ($x = 0.90$–1.0) oxides as cathode materials for intermediate-temperature solid oxide fuel cells," *International Journal of Hydrogen Energy*, vol. 39, no. 32, pp. 18392–18404, 2014.

[46] F. M. Aquino, D. M. A. Melo, R. C. Santiago et al., "Thermal decomposition kinetics of $PrMO_3$ (M = Ni or Co) ceramic materials via thermogravimetry," *Journal of Thermal Analysis and Calorimetry*, vol. 104, no. 2, pp. 701–705, 2011.

[47] F. Jin, H. Xu, W. Long, Y. Shen, and T. He, "Characterization and evaluation of double perovskites $LnBaCoFeO_{5+\delta}$ (Ln = Pr and Nd) as intermediate-temperature solid oxide fuel cell cathodes," *Journal of Power Sources*, vol. 243, pp. 10–18, 2013.

[48] R. Kannan, K. Singh, S. Gill, T. Fürstenhaupt, and V. Thangadurai, "Chemically stable proton conducting doped $BaCeO_3$ -No more fear to SOFC wastes," *Scientific Reports*, vol. 3, no. 1, pp. 1–5, 2013.

[49] A. A. Ansari, S. F. Adil, M. Alam et al., "Catalytic performance of the Ce-doped $LaCoO_3$ perovskite nanoparticles," *Scientific Reports*, vol. 10, no. 1, pp. 1–13, 2020.

[50] Z. Sun, W. Fan, Z. Liu, Y. Bai, Y. Geng, and J. Wang, "Improvement of dielectric performance of solid/gas composite insulation with YSZ/ZTA coatings," *Scientific Reports*, vol. 9, no. 1, pp. 1–12, 2019.

[51] J. Y. Huh, J. Lee, S. Z. A. Bukhari, J.-H. Ha, and I.-H. Song, "Development of TiO_2-coated YSZ/silica nanofiber membranes with excellent photocatalytic degradation ability for water purification," *Scientific Reports*, vol. 10, no. 1, pp. 1–12, 2020.

[52] X. Wang, H. Wang, and J. Shi, "Synthesis, characterization, and ceramic conversion of a liquid polymeric precursor to SiBCN ceramic via borazine-modified polymethylsilane," *Journal of Materials Science*, vol. 53, no. 16, pp. 11242–11252, 2018.

[53] S. Meyvel, P. Sathya, and G. Velraj, "Thermal characterization of archaeological pot sherds recently excavated in Nedunkur, Tamilnadu, India," *Cerâmica*, vol. 58, no. 347, pp. 338–341, 2012.

[54] A. M. Abdalla, S. Hossain, P. M. I. Petra, C. D. Savaniu, J. T. S. Irvine, and A. K. Azad, "Novel layered perovskite $SmBaMn_2O_{5+\delta}$ for SOFCs anode material," *Materials Letters*, vol. 204, pp. 129–132, 2017.

[55] X. Xu, J. Zhao, M. Li et al., "Sc and Ta-doped $SrCoO_{3-\delta}$ perovskite as a high-performance cathode for solid oxide fuel cells," *Composites Part B: Engineering*, vol. 178, p. 107491, 2019.

[56] J. H. Kim, Y. Kim, P. A. Connor, J. T. S. Irvine, J. Bae, and W. Zhou, "Structural, thermal and electrochemical properties of layered perovskite $SmBaCo_2O_{5+d}$, a potential cathode material for intermediate-temperature solid oxide fuel cells," *Journal of Power Sources*, vol. 194, no. 2, pp. 704–711, 2009.

[57] A. Tarancón, A. Morata, G. Dezanneau et al., "$GdBaCo_2O_{5+x}$ layered perovskite as an intermediate temperature solid oxide fuel cell cathode," *Journal of Power Sources*, vol. 174, no. 1, pp. 255–263, 2007.

[58] J.-H. Kim, F. Prado, and A. Manthiram, "Characterization of $GdBa_{1-x}Sr_xCo_2O_{5+\delta}$ ($0 \leq x \leq 1.0$) double perovskites as cathodes for solid oxide fuel cells," *Journal of the Electrochemical Society*, vol. 155, no. 10, p. B1023, 2008.